



## In-situ observation of a dendrite growth in an aqueous condition and a uranium deposition into a liquid cadmium cathode in an electrowinning system

Si-Hyung Kim <sup>\*</sup>, Dal-Seong Yoon, Young-Jae You, Seungwoo Paek, Joon-Bo Shim, Sang-Woon Kwon, Kwang-Rag Kim, Hong-Suk Chung, Do-Hee Ahn, Han-Soo Lee

Korea Atomic Energy Research Institute, P.O. Box 105, Yuseong, Daejeon 305-353, Republic of Korea

### A B S T R A C T

A zinc–gallium system was setup to observe the growth process of dendrites and to compare the performance of the stirrers which would prevent a dendrite formation. In a no-stirring condition, zinc was easily deposited on a liquid gallium cathode in the form of dendrites. It was difficult for a paddle stirrer to directly fracture the zinc dendrites to fine particles. However, a harrow stirrer was observed to fracture the dendrite to some extent at high speeds. Not only their rotation speed but also the length of their blades needed to be properly adjusted to enhance their performance. In the uranium–cadmium experiment, the diffusion coefficient of the uranium species was obtained by the cyclic voltammetry method, which is around  $1 \times 10^{-5} \text{ cm}^2/\text{s}$ . In a no-stirring condition, most of the uranium deposited at the current densities of 35, 100 and 200 mA/cm<sup>2</sup> did not sink into the liquid cadmium cathode.

© 2008 Elsevier B.V. All rights reserved.

### 1. Introduction

Korea atomic energy research institute (KAERI) has been developing pyrometallurgical techniques in four areas such as an electroreduction, an electrorefining, an electrowinning and a salt waste treatment. KAERI has used a consumable anode and a solid cathode for the electrorefining process whereas an inert anode and a liquid cathode have been used for the electrowinning process. In the case of the solid cathode, the gaps of the reduction potentials for uranium (U) and transuranic elements (plutonium, neptunium, americium, and curium) are so wide that U could be preferentially deposited on the cathode [1]. On the other hand, the differences in the reduction potentials of the elements are so narrow on the liquid cathode that transuranic elements could be simultaneously collected with the uranium [2–4]. Therefore, the electrolytic processes using liquid cathodes such as cadmium (Cd) or bismuth (Bi) have been studied in many countries [5–7].

During the co-deposition of U/TRU elements, however, the U ions are deposited in the form of dendrites [8] and these U dendrites are known to prevent a co-deposition of the U and TRU elements because the U dendrites with a large surface area float on the surface of the liquid cathode and play a role of a solid cathode. So, a paddle stirrer [9] and a pounder [7] were developed to hinder the formation of U dendrites on the liquid cathode in Japan and the United States, respectively.

Zinc (Zn) also has a tendency to form dendrites during the electrodeposition process. So, in the present work, a zinc–gallium (Ga) system [3] in an aqueous condition was setup to observe a dendrite growth behavior and to compare the performance of the stirrers which would hinder a dendrite formation. And, in the current U–Cd experiments, some basic data were obtained such as the diffusion coefficient of the U ions in LiCl–KCl electrolyte and the uranium deposition behavior, at some current densities, on the liquid Cd cathode without a stirring.

### 2. Experimental

#### 2.1. Zn–Ga system

Fig. 1 shows a schematic diagram of the Zn–Ga experimental apparatus, where Zn and Ga are simulated materials for U and Cd, respectively. The electrolyte container and cathode crucible were made of transparent acryl materials to visually observe the cathode reaction. A Zn plate (110 mm length, 90 mm height, 5 mm thickness) was positioned at one side of the electrolyte container and a cathode crucible (55 mm inner diameter, 40 mm depth) containing liquid Ga was located at the bottom of the electrolyte as shown in Fig. 1. About 350 g of liquid Ga was put into the cathode crucible.

Molybdenum (Mo) wires of 1 mm in diameter were used as electric leads for the Zn plate and the Ga cathode. A Pt wire with a diameter of 1 mm was used as a reference electrode. 1 M ZnSO<sub>4</sub> electrolyte solution was agitated at 100 rpm by a paddle stirrer

<sup>\*</sup> Corresponding author. Tel.: +82 42 868 2514; fax: +82 42 868 2990.  
E-mail address: [exodus@kaeri.re.kr](mailto:exodus@kaeri.re.kr) (S.-H. Kim).

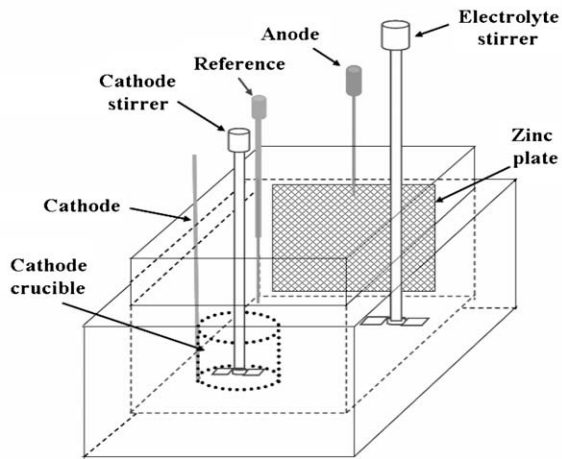


Fig. 1. Schematic diagram of the Zn–Ga system.

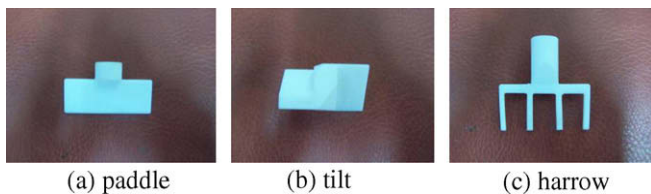


Fig. 2. Stirrer types.

with two blades (35 mm length, 15 mm height). Several kinds of stirrers such as paddle, tilt and harrow types, as shown in Fig. 2, were made and their performance was evaluated at rotation speeds of 40–150 rpm from the aspects of preventing a dendrite formation. The blade sizes of each cathode stirrer were 35–50 mm in length and 25 mm in height.

The electrolysis experiments were conducted to deposit Zn into the Ga cathode at 323 K and He gas was continuously purged to remove the oxygen incorporated in the electrolyte solution. The applied current was 2 A, which corresponds to a current density of 85 mA/cm<sup>2</sup> by assuming that the cathode surface area was equal to the inner diameter of the cathode crucible.

## 2.2. U–Cd system

Electrolysis experiments were carried out to recover the U contained in the LiCl–KCl molten salt (<99.99% purity) into the liquid Cd cathode at 773 K under a purified Ar atmosphere (less than 2 ppm of oxygen and 1 ppm of water). LiCl–KCl–UCl<sub>3</sub> salt mixtures of 140 g, where the amount of UCl<sub>3</sub> was 1.5–2 wt%, were put into an alumina salt crucible of 45 mm in inner diameter. Cd metal (99.999% purity) of about 10 g was contained in an alumina cathode crucible of 12 mm in inner diameter and 17 mm in depth. A stirrer with two blades was placed in the middle of the salt crucible and rotated at 60 rpm to mix the salt. No stirrer was used in the cathode crucible.

A Mo rod of 3 mm in diameter and a Mo wire of 1 mm in diameter were used as an anode and a cathode electrode, respectively. A silver–silver chloride (1 wt%AgCl in LiCl–KCl) electrode contained in a thin Pyrex glass tube was used as a reference. The cyclic voltammograms of the LiCl–KCl–UCl<sub>3</sub> salt were obtained at various potential scan rates of 20–300 mV/s and the electrodeposition experiments were conducted at current densities of 35, 100 and 200 mA/cm<sup>2</sup>.

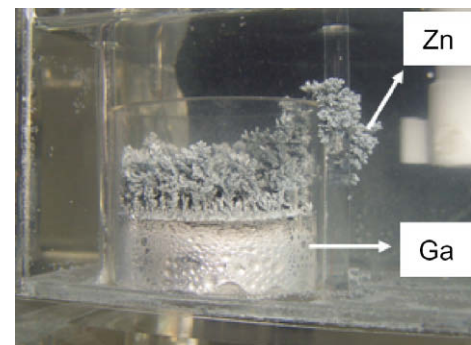
## 3. Results and discussion

### 3.1. 1. Zn–Ga system

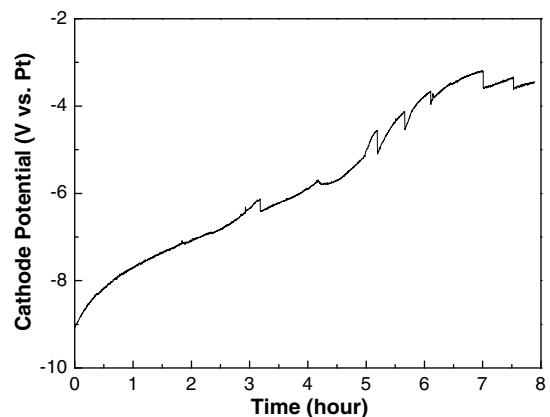
Zn is also known to be deposited in the form of dendrites [9] and the densities of Zn and Ga are about 7 g/cm<sup>3</sup> and 6 g/cm<sup>3</sup>, respectively. According to the Zn–Ga phase diagram, the solubility limit of Zn in liquid Ga is around 5 wt% at a reaction temperature of 323 K. All the experiments in this study were conducted using liquid Ga, fully saturated with Zn. In this case, the deposited Zn would begin to form a dendrite even from the beginning of a deposition.

Fig. 3 shows the Zn deposition results for the liquid Ga at a current density of 85 mA/cm<sup>2</sup> in a no-stirring condition of the liquid cathode. Deposits in the form of dendrites were seen to be created on the Ga surface (Fig. 3(A)). Those dendrites were grown vertically at first and then some of the dendrites were mounted over the top edge of the cathode crucible in the direction of the Zn anode, specifically toward the electrolyte stirrer. The tips of the dendrites grown out of the cathode crucible were continuously dropped to the bottom of the electrolyte container during the electrolysis experiment. A dendrite growth means not only an increase in the cathode area but also a shortening of the distance between the anode and the cathode, and thus the cathode potential decreases with the growth of the dendrite as shown in Fig. 3(b).

Fig. 4 shows the deposition results depending on the rotation speeds of the paddle stirrer. Commonly, all the cathode stirrers used in this study were positioned at the interface of the electrolyte and the liquid Ga. The change of the revolution speeds caused versatile deposition behaviors. The paddle stirrer rotating at 40 rpm merely swept the Zn deposits on the Ga surface and so the size of the depos-



(a) dendrite shapes after an electrolysis



(b) cathode potential change

Fig. 3. Zn deposition results for the Ga cathode in the no-stirring condition.

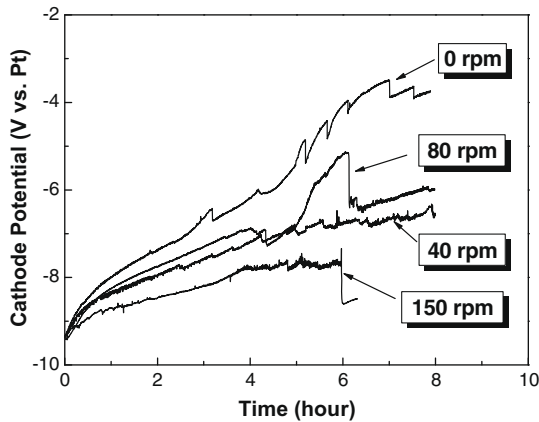


Fig. 4. Changes of the cathode potentials in the case of a paddle stirrer.

its became bigger with time. In the mean time, several deposits were crashed by colliding with each other. Through this process, the large deposits were smashed to small ones. As the speed increased to 80 rpm, Zn deposits were swept out toward the wall of the cathode crucible due to the centrifugal forces and thereby large zinc deposits were formed near the wall of the cathode crucible. It was observed that these large deposits collapsed around a reaction time of 6 h, which is predicted from the large peak of Fig. 4. At 150 rpm, some of the deposits overflowed out of the cathode crucible owing to the large centrifugal forces. Because of that, the cathode potential at 150 rpm was lower than that at slower rotation speeds. This overflow was not observed when using a shorter paddle stirrer. Therefore, it is considered that the lengths of the blades should be properly adjusted to prevent an overflow of the deposits. The tilt stirrers showed a similar performance as the paddle stirrers.

The harrow stirrer did not nearly prevent the dendrite growth at 40 rpm, which could be also predicted by the ascending curve at around 4 h in Fig. 5. But, at more than 100 rpm, it could hinder the dendrite growth well because the dendrite had a weak bonding force and could be crashed by harrow stirrer rotating at high speeds. In addition, the harrow stirrer did not bring about an overflow of the zinc deposits even at 150 rpm.

### 3.2. U–Cd system

#### 3.2.1. Diffusion coefficient

The cyclic voltammograms for the LiCl–KCl salt containing  $\text{UCl}_3$  were obtained with the Mo working electrode at various scanning rates (20–300 mV/s) at 773 K, which are shown in Fig. 6. The electro-

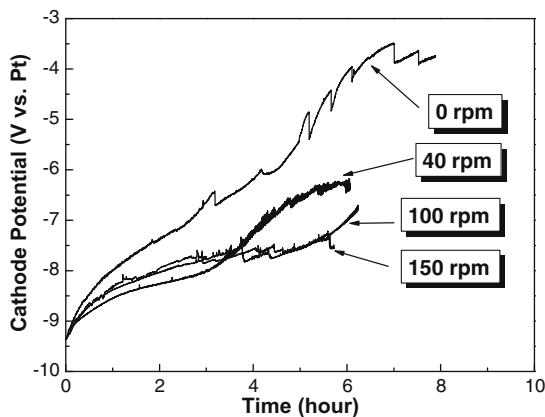


Fig. 5. Change of the cathode potentials depending on the rotation speeds with a harrow stirrer.

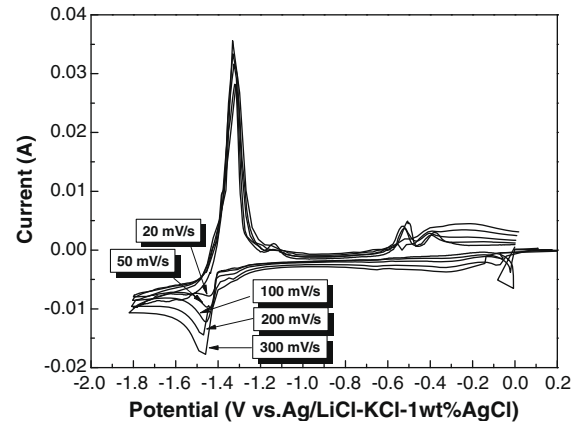


Fig. 6. Cyclic voltammograms of the  $\text{UCl}_3$  in LiCl–KCl at different scan rates at 773 K.

reduction of the  $\text{U}^{3+}$  ions proceeded at around  $-1.4$  V during the cathodic sweep and then the reduced U deposits were reoxidized from the cathode surface to the salt at around  $-1.32$  V during the anodic sweep. The cathodic peak potentials were independent of the scan rates up to 100 mV/s but shifted negatively for scan rates higher than 200 mV/s. The cathodic peak currents were directly proportional to the square root of the scan rates. The theory for the linear sweep voltammetry revealed that the electrode process was reversible and controlled by the diffusion of the reactant species for scan rates lower than 200 mV/s but became quasi-reversible after 200 mV/s [10].

The diffusion coefficient for the U (III) species was calculated by adapting the data obtained from the cyclic voltammetry to the Randles–Sevcik equation [11].

$$i_p = 0.61(nF)^{3/2}(RT)^{-1/2}AD^{1/2}Cv^{1/2}$$

where  $i_p$  is the cathodic peak current in amperes,  $n$  is the number of electrons involved in the reaction,  $F$  is the Faraday constant (96,485 C/mol),  $R$  is the gas constant (8.314 J/molK),  $T$  is the absolute temperature (K),  $A$  is the electrode surface area ( $\text{cm}^2$ ),  $D$  is the diffusion coefficient ( $\text{cm}^2/\text{s}$ ),  $C$  is the bulk concentration of the electroactive species ( $\text{mol}/\text{cm}^3$ ) and  $v$  is the potential scan rate (V/s). The U diffusion coefficient calculated by using this equation was about  $1 \times 10^{-5} \text{ cm}^2/\text{s}$  at 773 K, which agrees well with the results reported previously, that is,  $0.25\text{--}5 \times 10^{-5} \text{ cm}^2/\text{s}$  [12,13].

#### 3.2.2. Electrodeposition of U depending on the current densities in LCC

Fig. 7 shows the variation of the cathode potentials depending on the deposition time at each current density of 35, 100 and

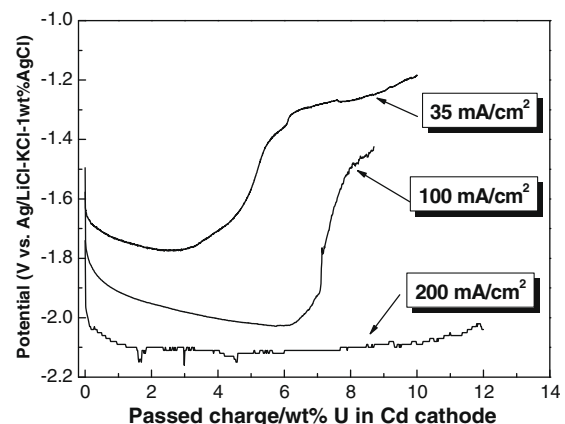


Fig. 7. Change of the cathode potentials as a function of the current densities.

200 mA/cm<sup>2</sup>. The passed charge of the x-axis was converted to a U weight ratio in the LCC by assuming that the U would be recovered at a current efficiency of 100%. When the electrodeposition experiments were carried out at 35 and 100 mA/cm<sup>2</sup>, the cathode potentials first fell and then rose rapidly. Similar tendencies were also observed at 200 mA/cm<sup>2</sup> even if the difference was decreased.

After the electrodeposition experiments were terminated, the cathode crucibles were taken out and then inspected visually to compare the appearances of the U deposits. Before these experiments, we predicted that U metals deposited at low current densities could sink under the liquid Cd surface even in the no-stirring condition because the U would not deposit in the form of a dendrite due to the low reduction rates. However, some of the U deposits in the experiments of 35 and 100 mA/cm<sup>2</sup> were grown out of the cathode crucible, as expected from the potential change in Fig. 7, in the direction of the anode, specifically toward the electrolyte stirrer as stated in the Zn–Ga system. And, U deposits were observed to flatly cover the Cd surface at 200 mA/cm<sup>2</sup>. It has been reported that the solubility limit of U in liquid Cd at 773 K is 2.35 wt% and the cathode potential is gradually shifted toward the negative direction until the liquid Cd is saturated with the U [2]. Koyama et al. [8] showed that a dendritic deposit growth was confirmed by a large cathode potential change in the cases of collecting U into LCC.

Our results showed that the uranium dendrite growth could not be prevented only by a cathode current density control. Therefore, further study will be conducted to develop stirrers for effectively hindering a uranium dendrite growth.

#### 4. Conclusions

As in the U–Cd system, the cathode potential curve for Zn–Ga also reflected a dendrite growth process well. It was difficult for a paddle stirrer to directly fracture the dendrite to fine particles. However, a harrow stirrer was observed to fracture the dendrite to some extent at high speeds. Not only the rotation speed but also

the length of their blades needs to be properly adjusted to enhance their performance.

The diffusion coefficient of the U(III) species was obtained from the cyclic voltammetry results, which is around  $1 \times 10^{-5}$  cm<sup>2</sup>/s. In the no-stirring condition, most of the U deposited at the current densities of 35, 100 and 200 mA/cm<sup>2</sup> did not sink into the liquid Cd because they had dendrite shapes. So, it is considered that the uranium dendrite growth can not be prevented only by a cathode current density control.

#### Acknowledgements

This study has been carried out under the Nuclear R&D Program by MOST (Ministry of Science and Technology) in Korea.

#### References

- [1] M. Iizuka, K. Uozumi, T. Inoue, T. Iwai, O. Shirai, U. Arai, J. Nucl. Mater. 299 (2001) 32.
- [2] K. Uozumi, M. Iizuka, T. Kato, T. Inoue, O. Shirai, T. Iwai, Y. Arai, J. Nucl. Mater. 325 (2004) 34.
- [3] J.J. Roy, L.F. Grantham, D.L. Grimmitt, S.P. Fusselman, C.L. Krueger, T.S. Storvic, T. Inoue, Y. Sakamura, N. Takahashi, J. Electrochem. Soc. 143 (1996) 2487.
- [4] S.P. Fusselman, J.J. Roy, D.L. Grimmitt, L.F. Grantham, C.L. Krueger, C.R. Nabelek, T.S. Storvic, T. Inoue, T. Hijikata, K. Kinoshita, Y. Sakamura, K. Uozumi, T. Kawai, N. Takahashi, J. Electrochem. Soc. 146 (1999) 2573.
- [5] T. Kato, T. Inoue, T. Iwai, Y. Arai, J. Nucl. Mater. 357 (2006) 105.
- [6] Y. Castrillejo, M.R. Bermejo, P.D. Arocas, A.M. Martinez, E. Barrado, J. Electrochem. Soc. 579 (2005) 343.
- [7] Argonne National Laboratory, CMT Annual Technical Report 1993, ANL-94/15, 1994.
- [8] T. Koyama, M. Iizuka, N. Kondo, R. Fujita, H. Tanaka, J. Nucl. Mater. 247 (1997) 227.
- [9] T. Koyama, M. Iizuka, Y. Shoji, R. Fujita, H. Tanaka, T. Kobayashi, M. Tokiwai, J. Nucl. Sci. Technol. 34 (4) (1997) 384.
- [10] A.J. Bard, L.R. Faulkner, *Electrochemical Methods. Fundamentals and Applications*, John Wiley, New York, 1980.
- [11] P. Delahay, In 'New Instrumental Methods in Electro-chemistry', Interscience Publishers, New York, 1954.
- [12] F. Caligara, L. Martinot, G. Duyckaerts, Bull. Soc. Chim. Belges. 76 (1967) 15.
- [13] P. Masset, R.J.M. Konings, R. Malmbeck, J. Serp, J.P. Galtz, J. Nucl. Mater. 344 (2005) 173.